GEM-Finder: dissecting GWAS variants via long-range interacting cis-regulatory elements with differentiation-specific genes

Gyeongsik Park[1*], Andrew J. Lee[1*] and Inkyung Jung[1†]

[1]Department of Biological Sciences, Korea Advanced Institute of Science and Technology (KAIST), Daejeon 34141, Republic of Korea

* These authors contributed equally to this work

[†]Correspondence: Inkyung Jung (ijung@kaist.ac.kr)

Abstract

Interpreting the functional significance of important variants identified by genome-wide association studies (GWAS) remains challenging, especially for those found in non-coding regions. Co-localizing these variants with cell-type specific *cis*-regulatory elements (CREs) has enhanced our understanding of their impact on gene regulation. However, a significant portion of non-coding variants are not associated with cell-type specific CREs, limiting their functional characterization. To tackle this challenge, we propose a novel analytical framework, Genomic Element Mapping for Fine Discovery of Promoter-Linked Variants (GEM-Finder). GEM-Finder utilizes long-range chromatin interactions to identify CREs that connect genes specific to each cell-type/differentiation-stage. Unlike conventional methods that mainly focus on cell-type/differentiation-specific CREs, GEM-Finder demonstrates superior performance by associating 7.6 times additional diseases/traits. Specifically, by integrating transcriptome, epigenome (particularly H3K27ac ChIP-seq), and long-range chromatin interactions during endothelial differentiation, we identified CREs linked to differentiation-specific genes. Our enrichment analyses revealed both shared and unique associations for 53 human diseases/traits. Notably, the majority of these (68%) exhibited unique associations in a differentiation-specific manner. Hematological traits and neuropsychiatric disorders were primarily linked to the final stage of endothelial differentiation, while several complex diseases, such as colorectal cancer (CRC), were unexpectedly associated with the late stage. Our findings underscore the importance of leveraging long-range chromatin interactions to accurately identify disease-associated CREs in the functional characterization of non-coding GWAS variants.

Introduction

The advent of genome-wide association studies (GWAS) has transformed our understanding of the genetic foundations of complex human diseases/traits (1). While these studies have identified numerous non-coding genetic variants associated with various conditions, interpreting the function of these variants remains a significant challenge, as the majority of GWAS variants reside in non-coding genomic regions (2). To address the gap between non-coding GWAS variants and their related molecular phenotypes, cis-regulatory elements (CREs), regulatory DNA sequences that can influence gene expression over long distances, have emerged as critical mediators of non-coding variant effects (3). CREs tightly control spatiotemporal gene regulation by modulating the transcriptional activities of target promoters through physical interactions (4,5,6). Therefore, disease-risk genetic variants found within cell-type specific CREs potentially alter specific transcription factor (TF) binding, consequently disrupting cell-type specific gene regulatory programs (7,8).

However, characterizing the regulatory impact of GWAS variants remains challenging, especially since many GWAS variants are not located within cell-type specific CREs, complicating the functional interpretation of these non-coding variants. To address this, we leveraged long-range chromatin interactions to identify CREs engaged with cell-type specific genes, enabling us to rescue additional CREs that harbor GWAS SNPs beyond just cell-type specific CREs. While there is a strong association between cell-type specific CREs and gene expression (9,10), a substantial number of shared CREs between cell-types are also linked to cell-type specific genes, suggesting that CREs physically connecting to specific

promoters via long-range chromatin interactions may provide more comprehensive and direct association with disease-specific target genes than those presenting solely cell-type specific activities. To test our hypothesis, we proposed a new analytical framework called Genomic Element Mapping for Fine Discovery of Promoter-Linked Variants (GEM-Finder).

We employed GEM-Finder to explore complex human diseases/traits associated with endothelial cells (ECs). ECs, which line the entire circulatory system, are essential for maintaining bodily homeostasis, including blood pressure regulation, immune cell trafficking, oxygen and nutrient transport, stem cell maintenance, and the creation of tissue-specific microenvironments (11,12,13,14). Endothelial dysfunction can impair vasodilation and promote a pro-inflammatory, pro-thrombotic state, leading to various pathological outcomes such as cardiovascular diseases, diabetes, and chronic renal failure (15,16,17). However, a systematic examination of GWAS variants about EC differentiation has yet to be conducted. By utilizing multi-omics approaches, incorporating transcriptome, epigenome, and 3D genome data, during EC differentiation, GEM-Finder successfully identified unique associations with various complex human diseases/traits at each differentiation stage. Notably, we observed unexpected enrichment of GWAS variants related to colorectal cancer within the gene regulatory program specific to late-stage ECs. In conclusion, GEM-Finder underscores the value of cell-type/differentiation specific long-range chromatin interactions in the functional characterization of GWAS variants.

RESULTS

3D genome reorganization coordinated with stage-specific gene expression and CRE activities during hESC-EC differentiation

To investigate whether 3D genome reorganization is involved in the dynamic gene regulation during endothelial differentiation from human embryonic stem cells (hESCs), we obtained multi-omics data, including transcriptome (RNA-seq), histone H3 lysine 27 acetylation (H3K27ac ChIP-seq), and 3D genome organization (Hi-C), from the GEO database (GSE201709) (**Fig. 1A and B**). In brief, the multi-omics data were generated by harvesting cells from hESCs, transitioning through the mesoderm stage by treating with GSK3β inhibitors for 72 hours and then inducing EC differentiation with VEGF-A and forskolin for 48 hours (18). Differentiating cells were collected at hESCs, mesoderm (ME), early (4hr), mid (12hr), late (24hr), and full (48hr) stages during EC specification and subjected to produce multi-omics results (**Fig. 1A**). This comprehensive dataset initially enabled us to identify a total of 136,967 CREs whit ChIP-seq data, by merging H3K27ac peaks from the individual samples. For each stage, we identified 22,180 hESC-specific, 19,063 mesoderm-specific, and 42,309 EC-specific CREs (6,493 for early, 6,920 for mid, 13,452 for late, and 15,444 for full differentiation stages).

Next, we examined the dynamic reorganization of the 3D genome structure during EC-differentiation (**Fig. 1B**). The analysis of compartment A/B patterns, an indicator of macro-scale 3D genome organization, illustrates substantial compartment transitions in both sides during EC differentiation **(Fig.1C).** Although overall relative ratio of compartment A and B is similar across each stage **(Fig. 1D),** tracing each region revealed that approximately 20% of the genome switches its compartment type **(Fig. 1E).** K-means clustering of genomic regions undergoing compartment switching revealed VEGF-A-dependent active compartment A regions, which progressively acquired during EC specification (**Fig. 1F**). Notably, these regions corresponded with upregulated gene expression and enhanced CRE activities (**Fig. 1G**). EC-progenitor (late or full stages) specific genes, such as *APLN* and *GAB1*, exhibited concordant changes between compartment A/B and gene expression, highlighting the functional role of the 3D genome organization in shaping the stage-specific transcriptome and epigenome relevant to EC specification (**Fig. 1H)**.

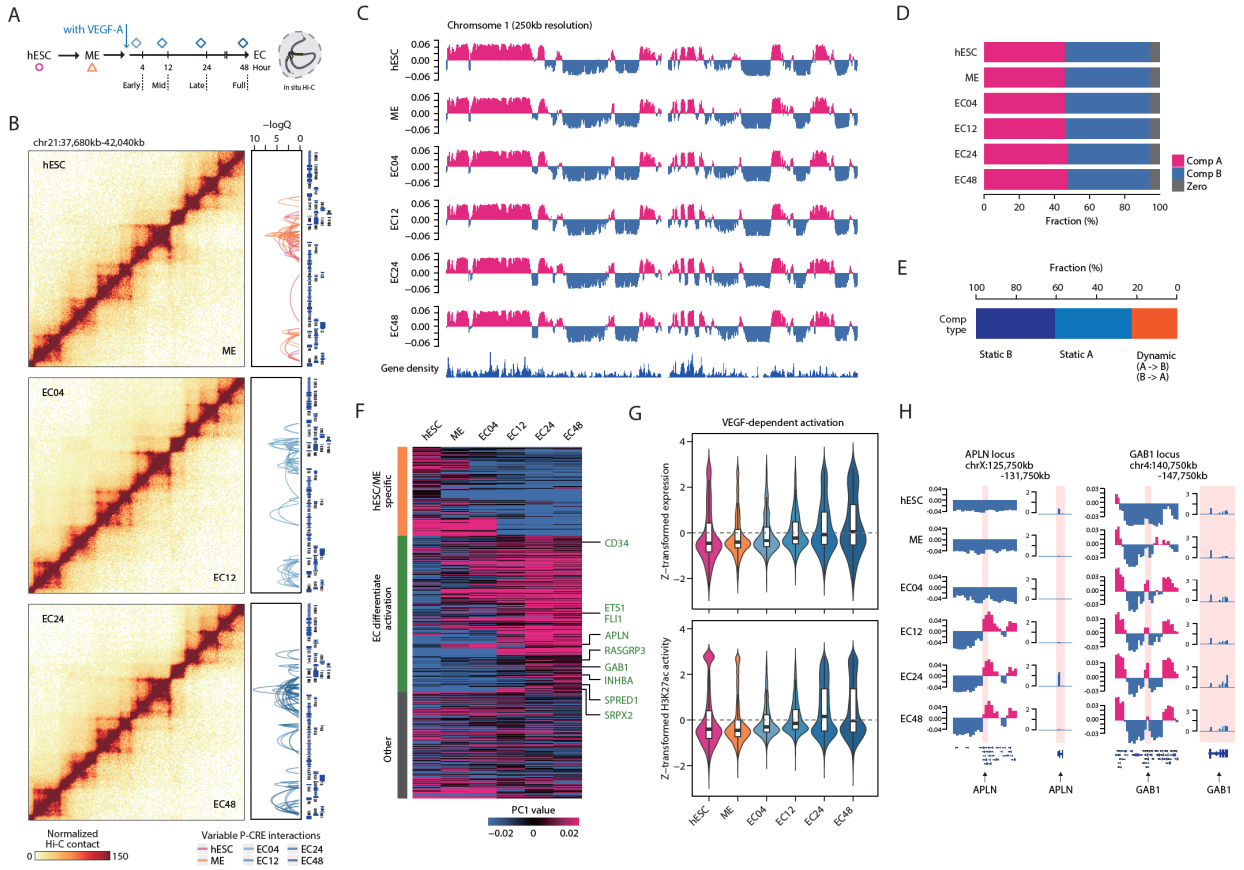

Fig. 1. Dynamic compartment A/B patterns during EC-differentiation. (A) A schematic overview of EC-differentiation. (**B**) Showing are Hi-C contact matrix and significant long-range interactions during EC-differentiation at x and 20kb resolution, respectively. **(C)** Shown are compartment A/B dynamics on chromosome 1 during EC-differentiation. (**D**) Stacked barplots showing the fraction of compartment A and B for each stage. (**E**) A stacked barplot showing the fraction of genomic regions subjecting to stable compartment A and B, and switching from A (or B) to B (or A). **(F)** K-mean clustering reveals hESC/ME specific and VEGF-A dependent compartment A regions. Representative genes resided in each cluster are shown together. (**G**) Violin plots showing gene expression patterns (top) and H2K27ac signals (bottom) along the EC-differentiation at VEGF-A dependent compartment A regions. **(H)** Genome browser snapshots for *APLN* and *GAB1* loci for compartment A/B patterns during EC-differentiation along with gene expression levels (TPM) at matched stage.

Stage-specific long-range chromatin interactions involve EC-specific CREs

Since long-range chromatin interaction is a key mechanism of gene regulation, we further explored the relationship between dynamic long-range chromatin interactions and EC differentiation-specific gene expression. Using Fit-HiC (19), we identified significant long-range chromatin interactions at a 0.01 FDR cutoff for each stage, with a resolution of 20kb (**Fig. 2A**). To determine variable and static long-range interactions, we included two non-EC cell types obtained during hESC differentiation without VEGF-A treatment (GSE201709). To account for variability in the number of identified interactions across differentiation stages due to variable Hi-C depth, we selected the same number of top-ranked long-range chromatin interactions for each stage. A total of 798,266 unique significant interactions were identified, with 74% being variable across multiple stages (**Fig. 2B**).

We further categorized these long-range interactions based on the presence of CREs at either or both anchors of the interacting regions (**Fig. 2C**). Consequently, 8.37% of long-range interactions were classified as promoter-CRE interactions, while 44.11% were categorized as CRE-other interactions. Next, we assessed whether variable promoter-CRE or CRE-other interactions were coordinated with stage-

specific CRE activities. Hypergeometric p-value test demonstrated significant overlap between the stage-specific CREs and variable long-range interactions (**Fig. 2D**). Our findings strongly support the idea that stage-specific long-range chromatin interactions, primarily linked by CREs, play a critical role in EC specification.

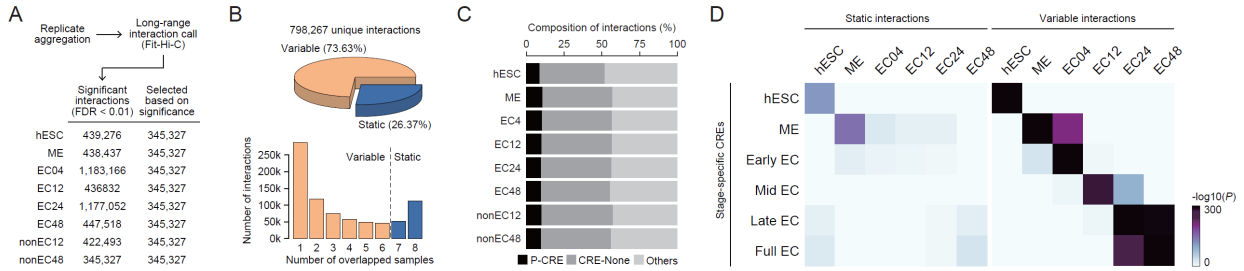

Fig. 2. Dynamic long-range chromatin interactions during EC-differentiation. (A) The number of identified significant interactions during EC-differentiation. **(B)** Shown are the fraction of variable and static long-range interactions (top) and the number of unique interactions in terms of the shared samples (bottom). (**C**) Barplots showing the fraction of promoter-CRE (p-CRE), CRE-other, and remaining interactions. **(D)** Heatmaps showing for hypergeometric p-values of the enrichment of EC-differentiation specific CREs at static (left) and variable (right) long-range chromatin interactions.

A development of GEM-Finder to link GWAS variants to CREs connecting stage-specific genes

Many recent studies have demonstrated that stage-specific CREs are crucial for characterizing non-coding genetic variants. Mapping GWAS variants to cell-type/differentiation specific CREs has significantly enhanced our understanding of complex human diseases/traits by identifying disease-relevant cell types and target genes of non-coding variants (20,21). However, a substantial portion of GWAS variants remains unexplained, as many are located outside of or in non-stage specific CREs. Additionally, not all cell-type or stage-specific CREs are linked to promoter regions, which limits the functional interpretation of CREs harboring GWAS variants.

To address these limitations, we hypothesized that analyzing candidate CREs connected to stage-specific genes through long-range chromatin interactions would provide greater insights into GWAS variants. To test our hypothesis, we proposed a new analytical framework called Genomic Element Mapping for Fine Discovery of Promoter-Linked Variants (GEM-Finder) (**Fig. 3A**). GEM-Finder consists of three steps: first, identifying candidate CREs using histone H3K27ac ChIP-seq or chromatin accessibility data; second, selecting candidate CREs that connect to cell-type or stage-specific gene promoters through long-range chromatin interactions; and third, conducting statistical enrichment tests for GWAS variants after LD expansion using permutation or LDSC regression analyses. We applied GEM-Finder to investigate associations between complex human diseases/traits and EC differentiation. We collected GWAS SNPs from 541 human diseases/traits, each with over 100 significant tag SNPs ($P < 5 \times 10^{-8}$). The enrichment analysis assessed the relationship between GWAS variants and stage-specific promoter-linked CREs based on linkage disequilibrium (LD; $r^2 > 0.8$), compared to random sets of simulated CREs (iterations = 1×10^5). The stage-specific promoter-linked CREs were derived from promoter-CRE long-range chromatin interactions of DEGs. For each stage, we identified approximately 8,500–36,000 DEG-contact CREs. Notably, using GEM-Finder, we identified 53 disease/trait associations in total during the EC differentiation stage through random permutation analyses (BHQ < 0.005 and fold change over expectation > 2), which is 7.6 times better than those identified by stage-specific CREs (7 diseases/traits are captured) (**Fig. 3B**).

To elucidate the enhanced performance of GEM-Finder, we examined how many stage-specific CREs are included in DEG-linked CREs. We found that only 10–30% were included, indicating that many stage-specific CREs identified by ChIP-seq data do not directly connect to stage-specific promoter regions (**Fig. 3C**). In addition, DEG-linked CREs revealed that only a small proportion was included without stage-specificity (**Fig. 3D**). Approximately 10–30% and 60–80% of CREs were uniquely defined or shared by other stages, respectively (**Fig. 3E**). Our results suggest that the strict standard for defining stage specific CREs could distinguish each stage well, but they couldn't effectively reflect stage-specific gene regulatory

programs due to loss of lots of information. The involvement of shared CREs in stage-specific DEGs may reflect complex gene regulatory programs.

Next, we examined the fraction of CREs co-localized with LD-expanded GWAS variants by GEM-Finder. We found that DEG-linked CREs displayed similar trends of GWAS variant enrichment across diseases/traits like stage-specific CREs, but a higher proportion of DEG-linked CREs were co-localized with GWAS variants (**Fig. 3F**). This result suggests that DEG-linked CREs may help mitigate false negatives from stage-specific analyses by leveraging long-range chromatin interactions and including additional DEG-linked CREs harboring GWAS variants.

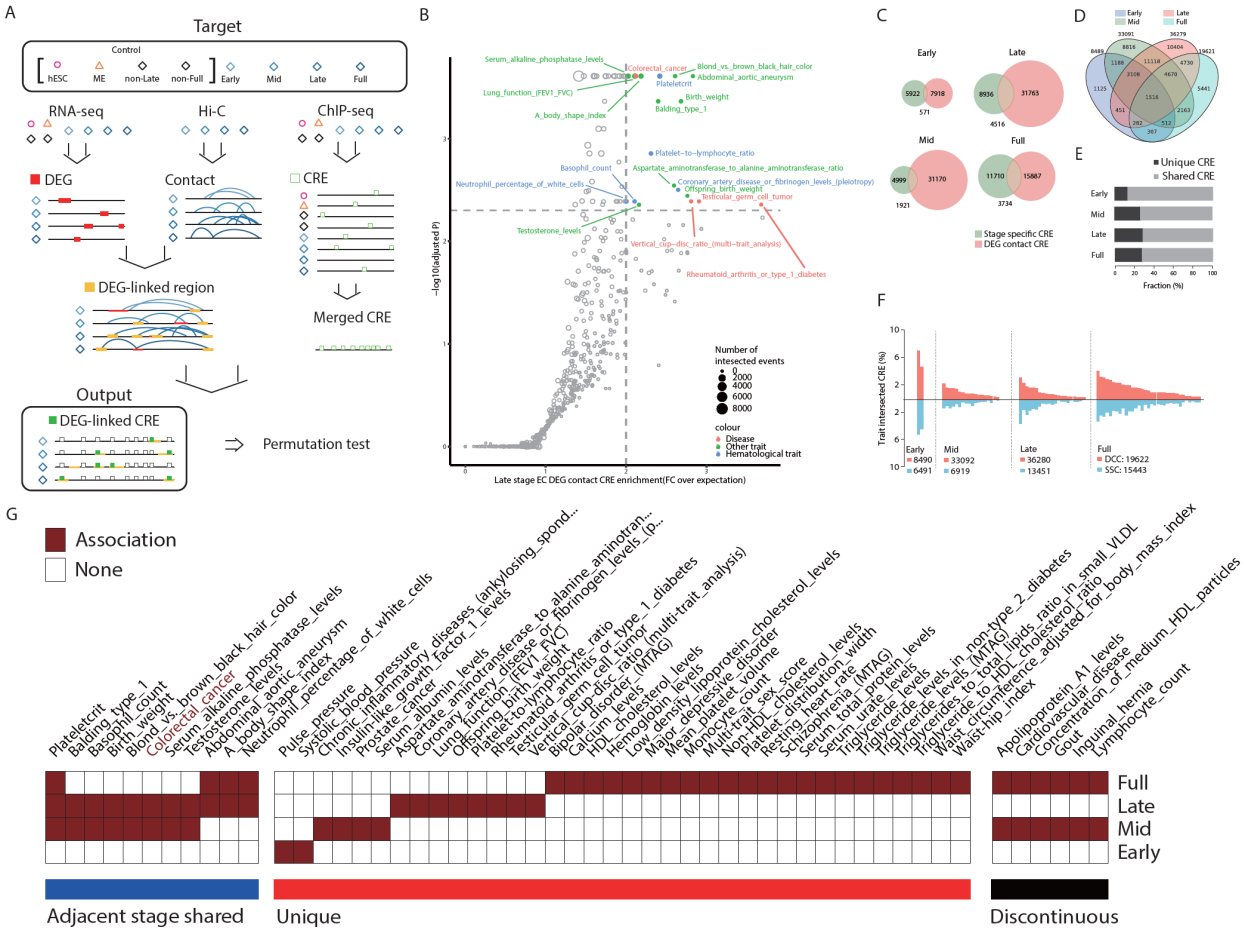

Fig. 3. Development of GEM-Finder and its application to EC-differentiation. (A) Overview of the GEM-Finder workflow. **(B)** Scatter plot presents permutation results with late stage DEG-linked CRE and 541 diseases/traits. Colored are significantly associated traits/diseases with Late EC. **(C)** Venn-diagrams show overlapping CREs between H3K27ac activity-based stage-specific CREs and DEG-linked CREs. **(D)** 4-circle Venn-diagram shows overlapping DEG-linked CREs among four differentiation stages. **(E)** Barplots highlight fractions of uniquely appeared DEG-linked CRE in each stage, and shared ones. **(F)** Bi-directional plots compare ratio of CREs harboring GWAS variants between stage specific CREs and DEG-linked CREs. **(G)** Heatmap represents associated stages of each disease/trait. Clustered by (1) shared by adjacent stages, (2) uniquely associated at specific stage, and (3) discontinuously associated at multi-stages.

When we focused on 53 significantly EC-associated diseases/traits, there were some notable findings (**Fig. 3G**). Take it for granted, many hematological traits, which are child traits of hematological measurement in the GWAS catalog, make significant associations with the EC, suggesting a significant role for EC-specific gene regulation in blood composition. In terms of stage-specific associations, we

categorized these diseases/traits into three groups: those shared by adjacent stages, uniquely associated traits, and those shared by discontinuous stages. Interestingly, 68% of EC-associated diseases/traits were uniquely linked to a specific differentiation stage, while the inclusion of adjacent stages accounted for 89% of the associations. In this organized result, we could get much information. For instance, only two traits are associated with the early stage, which are all blood pressure traits (pulse pressure and systolic blood pressure), and other 8 tested blood pressure related traits are not observed in other differentiation stages. This result suggests that the early stage-specific regulatory program will be a critical factor in determining the risk of blood pressure. The full stage showed associations not only with hematological properties but also with neuropsychiatric diseases and diabetes. The result aligns with recent studies highlighting potential blood-brain barrier dysfunctions in psychotic disorders (22,23). We also provided new biological insights by revealing a genomic link between EC differentiation and susceptibility to autoimmune disorders and colorectal cancer, evidenced by significant colocalization of EC-specific DEG-linked CREs with their respective GWAS variants (**Fig. 3G**). The overrepresentation of these traits and diseases in EC-specific gene regulation programs aligns with the physiological functions of the endothelium, as its dysfunction is likely to impact vascular function, immune cell trafficking, and tissue microenvironments (11,12,15,16). Overall, GEM-Finder provided more associations with complex human diseases/traits compared to conventional stage-specific CRE-based methods.

DISCUSSION

In this study, we developed GEM-Finder and applied it to multi-omics data (transcriptome, epigenome, and 3D genome) during endothelial cell (EC) differentiation, identifying stage-specific associations with complex human diseases/traits. GEM-Finder utilized long-range chromatin interactions and collected CREs connected to the genes with stage-specificity, revealing a novel insight into the genetic links between differentiation-dependent *cis*-gene regulatory networks and specific pathological dysfunctions. Unlike traditional methods that focus solely on differentiation-specific CREs, our approach enhances the ability to link a broader range of diseases/traits to GWAS variants. The significant increase in the number of associated complex diseases and traits highlights that both cell-type/differentiation-specific CREs and shared CREs are critical for the precise interpretation of GWAS variants. We also discovered numerous EC stage-specific associations for each disease, extending the previous understanding of cell-type associations to the level of cellular differentiation. Particularly, variants associated with colorectal cancer were exclusively enriched in late-stage-specific CREs, suggesting that tumor-associated endothelial cell (TEC) formation is closely linked to the "re-activation" of differentiated ECs, likely triggered by the hypoxic and high-VEGF-A tumor microenvironment.

Note that this framework is in an initial step, so lots of strategies could improve GEM-Finder's performance. Without delving into parameter and threshold optimization, it's clear that developing a novel prioritization method that incorporates both stage-specific CREs and DEG-linked CREs could further enhance the functional characterization of GWAS variants. Although there are few overlapped CREs between stage specific CREs and DEG-linked CREs **(Fig. 3C)**, the co-localization fractions of GWAS variants are quite similar **(Fig. 3F)**, suggesting that both groups contain cell type specific information. Given the complexity of the gene regulatory network, it is impossible to represent the entire cis-regulatory network for a given stage using only differentiation stage-specific CREs. Therefore, combining both CRE groups can help address false positive and false negative associations. To conclude, GEM-Finder clearly demonstrated the utility of long-range chromatin interactions for functional specification of non-coding variants associated with diverse human diseases/traits.

Materials and Methods

Identification of stage-specific DEGs and CREs in hESC-EC differentiation: We employed the quasi-likelihood F-test in EdgeR (26) to identify stage-specific DEGs associated with hESC-EC differentiation based on RNA-seq data. First, DEGs were identified by iteratively contrasting each of the distinct cell types (hESC, mesoderm, and EC) to the other cell types with a significance threshold of Benjamini-Hochberg (BH) corrected $P < 0.05$. Then, the samples at individual stages (early, mid, and late stage) of EC differentiation were iteratively compared to mesoderm to identify differentiation-dependent DEGs based on a significance threshold of BH corrected $P < 0.05$. Final DEG sets for individual stages are determined by

filtering their candidates with the absolute value of expression fold change > 1. This identical approach leveraging the quasi-likelihood F-test until BH correction, was taken to determine stage-specific CREs associated with hESC-EC differentiation based on H3K27ac ChIP-seq data. After BH correction, a stricter strategy to identify stage specific CREs is applied. We created a merged CRE set and assigned the differentiation stage and time-point at which the activity is the highest for each of the identified stage specific CREs.

***In situ* Hi-C data processing:** The sequencing output from Hi-C libraries was mapped to the reference genome (hg19) using BWA-mem (27) ('–M' option). In-house scripts were used to remove low quality reads (MAPQ < 10), the reads that span ligation sites, chimeric reads, and self-interacting reads (two fragments located within 5kb). The chimeric reads were removed since they are by-products of proximity ligation during Hi-C experiments, and cannot be properly processed by paired-end BWA-mem command. The read-pairs were merged as paired-end aligned BAM files and PCR duplicates were removed with Picard (v2.6.0). To evaluate contact-matrix similarity across Hi-C samples, stratum-adjusted correlation coefficients S The Hi-C contact matrices were generated in .hic file format by using juicer (28) and Knight-Ruiz normalization. The topologically associating domains (TADs) were systematically identified based on normalized 40kb resolution Hi-C contact maps by processing the directionality index (DI) scores (500kb window) with Domain Caller (29). Then, the genome was partitioned into TADs, boundaries, and unstructured regions. The unstructured regions were defined when the boundary was larger than 400 kb.

Compartment analysis: Identification of compartment A/B was performed similarly to an earlier work (30).

GEM-Finder framework: The key concept of GEM-Finder is defining DEG-linked CRE at each stage, reflecting differentiation-specific gene regulatory programs. To address our goal, processed transcriptome, epigenome (H3K27ac), and 3D genome data are applied in four steps: At first, merge individual stages' CREs to get DEG-linked CRE candidates. Second, annotate CREs and TSSs on all stages' significant Hi-C interaction data. Third, for each stage's annotated Hi-C data, extract interactions when one of the regions has DEG TSS. After that, for each stage's extracted interactions, collect TSS interacted CREs to make DEG-linked CRE. We treated this DEG-linked CRE as differentiation regulation regions, and applied GWAS heritability analysis to get EC differentiation stage-specific associated diseases/traits.

GWAS heritability analysis: GWAS-SNPs were obtained from the GWAS catalog database (All associations v1.0, downloaded on Aug. 2024) (31). The genomic coordinates for GWAS-SNPs were lifted to hg19 using the UCSC liftover tool and selected 541 human traits and diseases whose number of significant tag SNPs ($P < 5 \times 10^{-8}$) exceeds 100. The 360,079 representative genetic variants for the 541 GWAS traits were expanded using the linkage disequilibrium (LD) structure. LD scores were calculated using PLINK for five different populations, including African (AFR), American (AMR), East Asian (EAS), European (EUR), and South Asian (SAS), from 1000 genome phase 3 data. For each tag SNP, we identified associated SNPs that share a tight LD score ($r^2 > 0.8$) in at least two ethnic groups. To evaluate the statistical enrichment of GWAS-SNPs in target CREs, we considered the number of CREs in the input CREs group, that are associated with linkage disequilibrium expanded GWAS-SNPs and assessed the relative enrichment compared to the random expectation individually for selected human diseases/traits. For the random expectation, we generated a random set of genome coordinates that match the input CREs in number, size, and chromosomes. The enrichment was measured based on iterative trials ($n = 1 \times 10^5$) of random simulations and the statistical significance was calculated in the form of empirical *P*-value. This identified 53 human traits and diseases based on a significance threshold of BH corrected $P < 0.005$ and fold change over expectation > 2.

Acknowledgments: We thank the members of the Jung laboratory who provided support and suggestions throughout the course of this work. **Funding:** This study was supported by the Ministry of Science and ICT through the National Research Foundation in the Republic of Korea (2022R1A5A1026413, 2023R1A2C3002773, RS-2023-00223069, RS-2023-00262527). **Author contributions:** G.P., A.J.L. and I.J. designed and conceived the study. G.P. and A.J.L. analyzed and interpreted the results. S.M. and S.Y.J. conducted validation experiments. G.P. and A.J.L. prepared the manuscript with assistance from I.J. All authors read and approved the final manuscript. **Data and materials availability:** All raw sequencing data used in this study have been obtained from the GEO repository (GSE201709). Custom code supporting this work has been deposited in the GitHub repository (https://github.com/Delicate5/GEM-Finder). Any additional information required to reanalyze the data reported in this study is available from the lead contact upon request.

REFERENCES

1. Visscher, P.M., et al., 10 Years of GWAS Discovery: Biology, Function, and Translation. Am J Hum Genet, 2017. 101(1): p. 5-22.

2. Maurano, M.T., et al., Systematic localization of common disease-associated variation in regulatory DNA. Science, 2012. 337(6099): p. 1190-5.

3. Zhang, K., et al., A single-cell atlas of chromatin accessibility in the human genome. Cell, 2021. 184(24): p. 5985-6001 e19.

4. Jung, I., et al., A compendium of promoter-centered long-range chromatin interactions in the human genome. Nat Genet, 2019. 51(10): p. 1442-1449.

5. Martin, P., et al., Capture Hi-C reveals novel candidate genes and complex long-range interactions with related autoimmune risk loci. Nat Commun, 2015. 6: p. 10069.

6. Li, Y., et al., CRISPR reveals a distal super-enhancer required for Sox2 expression in mouse embryonic stem cells. PLoS One, 2014. 9(12): p. e114485.

7. Li, X., T. Lappalainen, and H.J. Bussemaker, Identifying genetic regulatory variants that affect transcription factor activity. Cell Genom, 2023. 3(9): p. 100382.

8. Lee, A.J., et al., Characterization of altered molecular mechanisms in Parkinson's disease through cell type-resolved multiomics analyses. Sci Adv, 2023. 9(15): p. eabo2467.

9. Zu, S., et al., Single-cell analysis of chromatin accessibility in the adult mouse brain. Nature, 2023. 624(7991): p. 378-389.

10. Li, Y.E., et al., A comparative atlas of single-cell chromatin accessibility in the human brain. Science, 2023. 382(6667): p. eadf7044.

11. Augustin, H.G. and G.Y. Koh, Organotypic vasculature: From descriptive heterogeneity to functional pathophysiology. Science, 2017. 357(6353).

12. Potente, M. and T. Makinen, Vascular heterogeneity and specialization in development and disease. Nat Rev Mol Cell Biol, 2017. 18(8): p. 477-494.

13. Gomez-Salinero, J.M. and S. Rafii, Endothelial cell adaptation in regeneration. Science, 2018. 362(6419): p. 1116-1117.

14. Aird, W.C., Endothelial cell heterogeneity. Cold Spring Harb Perspect Med, 2012. 2(1): p. a006429.

15. Rafii, S., J.M. Butler, and B.S. Ding, Angiocrine functions of organ-specific endothelial cells. Nature, 2016. 529(7586): p. 316-25.

16. Minami, T. and W.C. Aird, Endothelial cell gene regulation. Trends Cardiovasc Med, 2005. 15(5): p. 174-84.

17. Knapp, M., X. Tu, and R. Wu, Vascular endothelial dysfunction, a major mediator in diabetic cardiomyopathy. Acta Pharmacol Sin, 2019. 40(1): p. 1-8.

18. Patsch, C., et al., Generation of vascular endothelial and smooth muscle cells from human pluripotent stem cells. Nat Cell Biol, 2015. 17(8): p. 994-1003.

19. Ay, F., T.L. Bailey, and W.S. Noble, Statistical confidence estimation for Hi-C data reveals regulatory chromatin contacts. Genome Res, 2014. 24(6): p. 999-1011.

20. Li, Y.E., et al., A comparative atlas of single-cell chromatin accessibility in the human brain. Science, 2023. 382(6667): p. eadf7044.

21. Zhang, K., et al., A single-cell atlas of chromatin accessibility in the human genome. Cell, 2021. 184(24): p. 5985-6001 e19.

22. James, M.J., et al., An improved method for the preparation and culture of urothelial cells. J Urol, 1986. 136(5): p. 1141-2.

23. Stankovic, I., et al., Schizophrenia endothelial cells exhibit higher permeability and altered angiogenesis patterns in patient-derived organoids. Transl Psychiatry, 2024. 14(1): p. 53.

24. Meyer, D., et al., Significance of dinucleoside tetraphosphate production by cultured tumor cells exposed to the presence of ethanol. Biochimie, 1990. 72(1): p. 57-64.

25. Yang, D., et al., RasGRP3 contributes to formation and maintenance of the prostate cancer phenotype. Cancer Res, 2010. 70(20): p. 7905-17.

26. Robinson, M.D., D.J. McCarthy, and G.K. Smyth, edgeR: a Bioconductor package for differential expression analysis of digital gene expression data. Bioinformatics, 2010. 26(1): p. 139-40.

27. Li, H. and R. Durbin, Fast and accurate long-read alignment with Burrows-Wheeler transform. Bioinformatics, 2010. 26(5): p. 589-95.

28. Durand, N.C., et al., Juicer Provides a One-Click System for Analyzing Loop-Resolution Hi-C Experiments. Cell Syst, 2016. 3(1): p. 95-8.

29. Dixon, J.R., et al., Topological domains in mammalian genomes identified by analysis of chromatin interactions. Nature, 2012. 485(7398): p. 376-80.

30. Dixon, J.R., et al., Chromatin architecture reorganization during stem cell differentiation. Nature, 2015. 518(7539): p. 331-6.

31. Sollis, E., et al., The NHGRI-EBI GWAS Catalog: knowledgebase and deposition resource. Nucleic Acids Res, 2023. 51(D1): p. D977-D985.